J|A|C|S COMMUNICATIONS

Published on Web 05/14/2009

Synthesis and Oxygen Reduction Electrocatalytic Property of Pt-on-Pd Bimetallic Heteronanostructures

Zhenmeng Peng and Hong Yang*

Department of Chemical Engineering, University of Rochester, Gavett Hall 206, Rochester, New York 14627

Received March 22, 2009; E-mail: hongyang@che.rochester.edu

One key area in advancing hydrogen fuel cells is to improve both the sluggish kinetics and long-term stability of cathode catalysts.[1−3] A major strategy for improving the activity is to use platinum alloys instead of pure platinum as the electrocatalysts,[4] though leaching of nonplatinum metal over time is a major issue. The loss of surface area due to Ostwald ripening or grain growth is another major factor that often results in the degradation of catalytic performance.[5] One solution to improve the durability is to deposit Au nanoclusters on Pt catalysts.[6]

In this paper, we describe a new approach to address both the activity and stability issues synergistically by using palladium metal nanoparticles as support for Pt catalysts based on a particle-on-particle structure. Such heterogeneous bimetallic nanocrystals are expected to integrate several different functionalities in one structure, which is difficult to accomplish in a single-component material. The rationales for choosing palladium as a metallic support for platinum nanoparticles are based on the following two major factors: First, both metals have a face-centered cubic (*fcc*) phase with a unit length of 3.92 Å for Pt and 3.89 Å for Pd. The small lattice mismatch means that the epitaxial growth should be favored.[7] Second, a Pt monolayer on a Pd surface shows significantly higher catalytic activity than pure Pt in an oxygen reduction reaction (ORR).[8]

Selective growth of metals on semiconductors and metal oxides and semiconductors on semiconductors has been investigated in recent years, though examples on well-defined metal-on-metal heteronanostructures are still quite limited.[7,9−11] Heterogeneous nucleation and growth, however, should be favored thermodynamically over the homogeneous nucleation for the corresponding individual elements, when the global energy minimum is dominated by interfacial energy.[3,12] Additional reduction in free energy can further be achieved through epitaxial growth. Here we report the synthesis of Pt-on-Pd heterogeneous bimetallic nanostructures based on such principles. Carbon-supported Pt-on-Pd bimetallic nanostructures are further examined for its catalytic properties in ORR.

The Pt-on-Pd nanoparticles were prepared using a sequential synthetic method (See Supporting Information for details). The palladium nanoparticles were made from palladium acetylacetonate in oleylamine based on a modified procedure.[13,14] The as-made palladium nanoparticles were fairly monodisperse and had an average diameter of 5.3 ± 0.6 nm (Figure S1). A powder X-ray diffraction (PXRD) pattern shows the particles were made of Pd metal (Figure S2). Figure 1a shows the representative TEM image for the as-synthesized Pt-on-Pd nanoparticles. The Pt nanoparticles had an average diameter of ∼3 nm and were distributed evenly on the surface of palladium nanoparticles. A high-resolution TEM (HR-TEM, FEI TECNAI F-20) image shows that these nanoparticles have good crystallinity with well-defined fringes (Figure 1b). The Pt nanoparticles grew along the (111) crystal planes on Pd supports. No obvious grain boundaries or defects could be observed, as only a very small lattice mismatch of 0.77% existed between Pt and Pd metals.[7] Similar architectures have been reported in other bimetallic systems, such as Au−Pt.[11] The elemental distributions of these two metals were studied by high-angle annular dark field scanning TEM (HAADF-STEM). Figure 1c−e show a representative STEM image and the corresponding energy dispersive X-ray (EDX) maps for Pd and Pt of a Pt-on-Pd nanoparticle. While Pd could only be detected in the core region, Pt was found throughout the entire particle including the "branch" regions, indicating the formation of Pt-on-Pd nanoparticles. A PXRD pattern shows multiple diffraction peaks could be observed and indexed to an *fcc* lattice (Figure S2). The atomic ratio between Pd and Pt in the bimetallic nanostructures was ∼1/3 based on the EDX analysis using field emission scanning electron microscopy (FE-SEM, Zeiss-Leo DSM982), close to the Pd metal/Pt(acac)$_2$ molar ratio in the reaction mixture (Figure S3). The as-made nanoparticles could be loaded onto a carbon support (Vulcan XC-72R) and thermally treated to make Pt-on-Pd bimetallic catalysts. Figure 1f shows representative TEM images of carbon-supported Pt-on-Pd nanoparticles at 20 wt % loading of metals. The Pt-on-Pd nanoparticles were still evenly distributed on carbon supports without obvious sintering or growth of particles after thermal treatment. HR-TEM study and EDX maps show the particle-on-particle morphology and elemental distributions remained largely intact (Figure 1g and Figure S4a−c). The

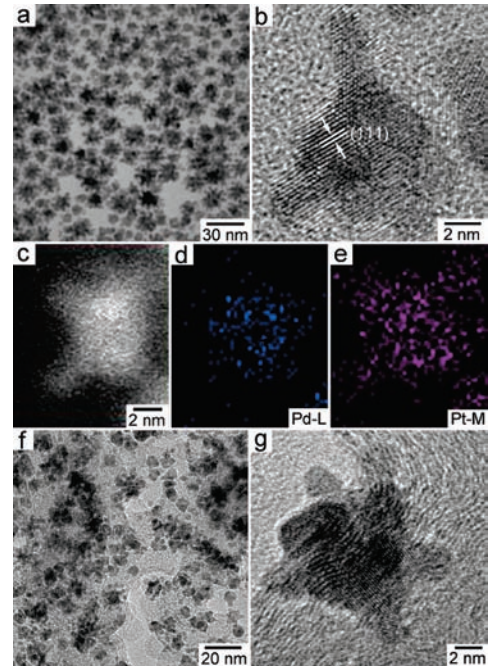

Figure 1. Representative (a) TEM, (b) HR-TEM, (c) HAADF-STEM images and (d, e) elemental maps for Pd and Pt metals of Pt-on-Pd bimetallic nanoparticles; (f) TEM and (g) HR-TEM images of carbon-supported Pt-on-Pd bimetallic catalysts after the thermal treatments.

10.1021/ja902256a CCC: $40.75

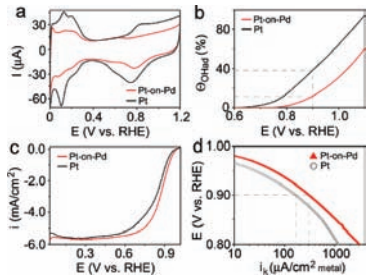

Figure 2. (a) CV, (b) hydroxyl surface coverage (Θ_{OH}), (c) ORR polarization curves, and (d) specific kinetic current densities (i_k) for carbon-supported Pt-on-Pd and Pt catalysts.

PXRD diffraction peaks became slightly sharper than before (Figure S4d), indicating an improvement in crystallinity.

Figure 2 shows the electrochemical properties of carbon-supported Pt-on-Pd heteronanostructure and Pt reference catalysts (E-TEK, 20 wt % Pt, diameter: 2.5 nm) (See Supporting Information for details). The electrochemical surface area (ECSA) for the Pt-on-Pd catalyst was found to be 37.3 m^2/g metal (or 44.5 m^2/g Pt) based on the cyclic voltammetry (CV) data (Figure 2a). Well-defined chemical adsorption peaks of hydrogen on different Pt low-index surfaces became less definable for the Pt-on-Pd catalyst. The incorporation of Pd also greatly altered the ability to absorb hydroxyl species (OH_{ad}, $E > 0.6$ V) (Figure 2b). Both the onset and peak potentials for the Pt-on-Pd catalyst had positive shifts in comparison with pure Pt on the backward sweep, suggesting the fast hydroxyl desorption from the Pt-on-Pd surfaces. The ORR tests were conducted in O_2-saturated $HClO_4$ aqueous solutions at an ECSA of 2.0 cm^2 for all catalysts on a glass carbon electrode (GCE). Figure 2c shows the polarization curves for both carbon-supported Pt-on-Pd and pure Pt catalysts. The Pt-on-Pd catalysts exhibited a more positive on-set potential and higher activity than the pure Pt nanoparticles. The area-specific current density (i_k), which represents the intrinsic activity of the catalysts and calculated using Koutecky−Levich equation,[15] was 307 μA/cm^2 Pt at 0.9 V for the Pt-on-Pd nanostructures and nearly doubled that for the Pt catalyst (166 μA/cm^2 metal) (Figure 2d). These results agreed well with those reported for Pt skin layers on Pd surfaces.[8] The adsorbed OH_{ad} species has a negative impact on the ORR and low OH_{ad} coverage on the surface of Pt-on-Pd catalysts helps improve the kinetics, thus enhancing the activities.[3,8]

The long-term stability of the Pt-on-Pd catalyst was evaluated by applying linear potential sweeps between 0.6 and 1.0 V based on an established procedure.[5a,6] After 30 000 cycles, Pt-on-Pd catalysts lost ~12% of the initial ECSA (Figure 3a) and showed a small degradation of 9 mV in the half-wave potential (Figure 3b). The particle-on-particle morphology, size, and even composition remained after the accelerated tests (Figure S5). In sharp contrast, the degradation of Pt catalyst was quite serious, with a loss of 39% of the initial ECSA and a large decrease of 35 mV in the half-wave potential after the test (Figure 3c−d). The Pt nanoparticles also experienced a dramatic growth in diameter after the cycles, changing from 2.5 to 3.9 nm (Figure S6). The much improved stability thus could be due to the favored interfacial structures between Pt and Pd supports, as well as the larger than usual overall particle size of Pt-on-Pd nanostructures, which prevented the small Pt from dissolution in the ORR. This platinum-on-metal architecture provides a new design strategy for making hydrogen fuel cell cathode catalysts with both excellent activity and stability.

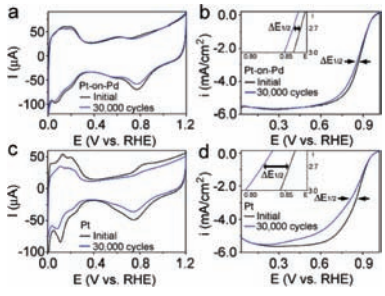

Figure 3. CV and ORR polarization curves for carbon-supported (a, b) Pt-on-Pd and (c, d) Pt catalysts before and after 30 000 cycles.

Acknowledgment. This work is supported by the NSF (DMR-0449849). It made use of Shared Facilities at University of Rochester River Campus EM Lab supported in part by the DOE.

Supporting Information Available: Detailed synthesis and characterization procedures. Figures S1−S6 contain TEM, XRD, EDX, electrochemical activity, and stability data. This material is available free of charge via the Internet at http://pubs.acs.org.

References

(1) (a) Gasteiger, H. A.; Kocha, S. S.; Sompalli, B.; Wagner, F. T. *Appl. Catal., B* **2005**, *56*, 9–35. (b) de Bruijn, F. A.; Dam, V. A. T.; Janssen, G. J. M. *Fuel Cells* **2008**, *8*, 3–22.
(2) Chen, G. Y.; Delafuente, D. A.; Sarangapani, S.; Mallouk, T. E. *Catal. Today* **2001**, *67*, 341–355.
(3) Peng, Z. M.; Yang, H. *Nano Today* **2009**, *4*, 143–164.
(4) (a) Stamenkovic, V. R.; Fowler, B.; Mun, B. S.; Wang, G. F.; Ross, P. N.; Lucas, C. A.; Markovic, N. M. *Science* **2007**, *315*, 493–497. (b) Koh, S.; Strasser, P. *J. Am. Chem. Soc.* **2007**, *129*, 12624–12625. (c) Chen, S.; Ferreira, P. J.; Sheng, W. C.; Yabuuchi, N.; Allard, L. F.; Shao-Horn, Y. *J. Am. Chem. Soc.* **2008**, *130*, 13818–13819. (d) Stamenkovic, V.; Schmidt, T. J.; Ross, P. N.; Markovic, N. M. *J. Phys. Chem. B* **2002**, *106*, 11970–11979.
(5) (a) Ferreira, P. J.; la O, G. J.; Shao-Horn, Y.; Morgan, D.; Makharia, R.; Kocha, S.; Gasteiger, H. A. *J. Electrochem. Soc.* **2005**, *152*, A2256–A2271. (b) Shao, Y. Y.; Yin, G. P.; Gao, Y. Z. *J. Power Sources* **2007**, *171*, 558–566. (c) Yu, X. W.; Ye, S. Y. *J. Power Sources* **2007**, *172*, 145–154.
(6) Zhang, J. L.; Sasaki, K.; Sutter, E.; Adzic, R. R. *Science* **2007**, *315*, 220–222.
(7) (a) Habas, S. E.; Lee, H.; Radmilovic, V.; Somorjai, G. A.; Yang, P. *Nat. Mater.* **2007**, *6*, 692–697. (b) Lee, H. J.; Habas, S. E.; Somorjai, G. A.; Yang, P. D. *J. Am. Chem. Soc.* **2008**, *130*, 5406–5407.
(8) (a) Zhang, J. L.; Mo, Y.; Vukmirovic, M. B.; Klie, R.; Sasaki, K.; Adzic, R. R. *J. Phys. Chem. B* **2004**, *108*, 10955–10964. (b) Zhang, J. L.; Vukmirovic, M. B.; Xu, Y.; Mavrikakis, M.; Adzic, R. R. *Angew. Chem., Int. Ed.* **2005**, *44*, 2132–2135.
(9) (a) Mokari, T.; Rothenberg, E.; Popov, I.; Costi, R.; Banin, U. *Science* **2004**, *304*, 1787–1790. (b) Mokari, T.; Sztrum, C. G.; Salant, A.; Rabani, E.; Banin, U. *Nat. Mater.* **2005**, *4*, 855–863. (c) Yu, H.; Chen, M.; Rice, P. M.; Wang, S. X.; White, R. L.; Sun, S. H. *Nano Lett.* **2005**, *5*, 379–382. (d) Cozzoli, P. D.; Manna, L. *Nat. Mater.* **2005**, *4*, 801–802. (e) Gu, H. W.; Zheng, R. K.; Zhang, X. X.; Xu, B. *J. Am. Chem. Soc.* **2004**, *126*, 5664–5665. (f) Yang, J.; Elim, H. I.; Zhang, Q. B.; Lee, J. Y.; Ji, W. *J. Am. Chem. Soc.* **2006**, *128*, 11921–11926.
(10) Milliron, D. J.; Hughes, S. M.; Cui, Y.; Manna, L.; Li, J. B.; Wang, L. W.; Alivisatos, A. P. *Nature* **2004**, *430*, 190–195.
(11) (a) Peng, Z. M.; Yang, H. *Nano Res.* **2009**, *2*, 406–415. (b) Zhou, S. G.; McIlwrath, K.; Jackson, G.; Eichhorn, B. *J. Am. Chem. Soc.* **2006**, *128*, 1780–1781.
(12) (a) Roder, H.; Schuster, R.; Brune, H.; Kern, K. *Phys. Rev. Lett.* **1993**, *71*, 2086–2089. (b) Wilcoxon, J. P.; Provencio, P. P. *J. Am. Chem. Soc.* **2004**, *126*, 6402–6408. (c) Chambers, S. A. *Surf. Sci. Rep.* **2000**, *39*, 105–180.
(13) Kim, S. W.; Park, J.; Jang, Y.; Chung, Y.; Hwang, S.; Hyeon, T.; Kim, Y. W. *Nano Lett.* **2003**, *3*, 1289–1291.
(14) Liu, Q. S.; Bauer, J. C.; Schaak, R. E.; Lunsford, J. H. *Angew. Chem., Int. Ed.* **2008**, *47*, 6221–6224.
(15) (a) Bard, A. J.; Faulkner, L. R. *Electrochemical Methods - Fundamentals and Application*, 2nd ed.; John Wiley & Sons:New York, 2001. (b) Vielstich, W.; Lamm, A.; Gasteiger, H. A. *Handbook of Fuel Cells, Fundametnals Technology and Applications*; John Wiley & Sons Ltd.: 2003; Vol. 2.

JA902256A